Investigation and Simulation of Catalytic Reforming Reactions of Iraqi Heavy Naphtha Using Pt-Sn/AL_2O_3 and Pt-Ir/AL_2O_3 Catalysts

Khalid A.Sukkar, Shahrazad R.Raouf, and Ramzy S.Hamied

Khalid A.S., Ass. Proof, Khalid_ajmee@yahoo.co, Pet Tech Dep, University of Technology / Iraq.

Shahrazad R.R., Ass. Proof, srraouf@yahoo.uk.co, Chem. Eng Dep, University of Technology / Iraq.

Ramzy S.H., Dr, ramze_eng@yahoo.co, Pet Tech Dep, University of Technology / Iraq.

Abstract

In present study: experimental and simulation studies have been carried out to describe the reaction kinetics of catalytic reforming process using Iraqi heavy naphtha as a feedstock for the process. Two types of bi-metals catalysts were prepared (Pt-Sn/AL_2O_3 and Pt-Ir/AL_2O_3) supported on γ-AL_2O_3.

The main three described reforming reactions were investigated (dehydrogenation, dehydrocyclization, and hydrocracking) to characterize catalysts performance in term of activity and selectivity. The performances of catalysts were investigated under the following operating condition: reaction temperature range of 480-510 ˚C, weight hour space velocity range of 1-2hr^{-1}, pressure at 6 atm, and hydrogen to hydrocarbon ratio of 4:1.

The results show higher conversion of Iraqi heavy naphtha components (i.e., Paraffins and Naphthenes) with higher temperatures where as, weight hourly space velocity has shown negative impact on conversion (i.e., higher WHSV shows lower conversion). In general, it was noted that the yields of aromatics and high components are increased for both types of catalysts (Pt-Sn/AL_2O_3 and Pt-Ir/AL_2O_3) under the same operating conditions.

A comprehensive mathematical model and simulation was developed in the present work to describe the reaction kinetics of reforming reactions. The comparison between the concentration of (Paraffin's, Naphthenes, and Aromatics), and temperature profile of experimental and simulation results showed a good agreement with a deviation confined between 1.93% to 14.51%.

Key words: Experimental and Simulation; catalytic reforming; Pt-Sn/AL_2O_3 and Pt-Ir/AL_2O_3 catalysts.

Introduction

Catalytic reforming of heavy naphtha is a very important process for producing high octane gasoline, aromatic feedstock and hydrogen in petroleum-refining and petrochemical industries. Catalytic naphtha reforming is the process which converts low octane compound in naphtha to high-octane gasoline components, without changing carbon numbers in the molecule. This is achieved mainly by conversion of straight chain naphtha to iso-paraffins and aromatics over a solid catalyst [1].

During catalytic reforming long chain hydrocarbons are rearranged through isomerization, hydrogenation, dehydrocyclization and dehydrogenation reactions. These reactions occur on acid and/or metal sites and they demand the use of bifunctional catalysts. The acid function is typically provided by a solid support such as chlorinated alumina (Al_2O_3–Cl) and the metal function by a noble metal. The metal component is active for the hydrogenation and dehydrogenation reactions while the support has the acid strength necessary to promote the isomerization reactions. Synergetic action of both kinds of active sites promotes other reactions such as dehydrocyclization via a bifunctional reaction mechanism. Undesirable reactions such as hydrocracking and hydrogenolysis also occur lowering the yield of valuable products and deactivating the catalyst by the formation of coke on the active sites [2, 3].

The metals used with Pt/ Al_2O_3 catalyst other than Re are Sn, Ge, and Ir. These additives modify the activity, selectivity and stability of the catalyst. These metals are used as bimetallic catalyst. The effects of the additives on the reforming reaction are:

(I) They decrease the deep dehydrogenation capacity of (Pt) and thus decrease the formation of unsaturated coke precursors.

(II) They decrease the hydrogenolysis capacity and therefore also decrease the formation of light gases.

(III) They modify the concentration of surface hydrogen. This has an effect on relative production of different reaction intermediates and therefore on the final reaction selectivity.

(IV) A portion of the additives remains oxidized on the surface and modifies the amount and strength of the acid site of the support.

This type of bimetallic naphtha reforming catalyst makes a big leap forward in the technology of reforming catalyst and it improves its properties, Pt-Ir/ Al_2O_3-Cl, Pt-Sn/ Al_2O_3-Cl, and Pt-Ge/ Al_2O_3-Cl being the most remarkable followers [4, 5].

Recently there has been a renewed interest in the reforming process, first, because reformat is a major source of aromatics in gasoline, and second, because of the new legislation concerning benzene and aromatics content in commercial gasoline. In this sense, reformers have reduced the severity of the industrial reforming plants in order to decrease the amount of aromatics in gasoline; however it adversely affects the octane. Therefore, to design new plants and optimize the existing ones, an appropriate mathematical model for simulating the industrial catalytic reforming process is needed. [6, 7]. The aim of this work is to produce high octane aromatics with adding hydrogen from Iraqi heavy naphtha by using prepared bi-metallic catalysts in a fixed bed reactor with various ranges of temperatures and weight hour space velocity. A mathematical model has been a developing to describe the catalytic reforming reactions, reaction rate and optimum operating conditions for the reforming catalysts.

2. Experimental Work

2.1 Materials

2.1.1 Naphtha feedstock

Iraqi heavy naphtha with 0.733 specific gravity was supplied by Al-Dura refinery. The properties of this naphtha are tabulated as represent in Table (1).

2.1.2 Gases

Nitrogen purchased from Dijlah factory, was analyzed by G.C and confirms its purity of 99%. G.C analysis for purchased from Al-Mansor plant, shows that its purity of 99.9%. To reduce oxygen and water impurities an molecular sieve type (5A) has been installed on the hydrogen line.

2.1.3 Catalysts and Support

Pt/ γ-Al_2O_3 (RG 412), Pt-Re/ γ-Al_2O_3 (RG 482) catalysts are supplied from Al-Dura refinery. The two bi-metals catalysts were prepared in our laboratory. The physical and chemical properties of all catalysts are given in Table (2):

2.2Preparation of Bi-Metal Catalyst

2.2.1 Preparation of Platinum-Iridium / Alumina Catalyst

The Pt-Ir/Al_2O_3 catalyst was prepared by impregnation the parent catalyst (Pt/Al_2O_3) with Iridium chloride ($IrCl_3$) in order to reach final concentration of 0.5 wt% of Pt and 0.1 wt% of Ir [8].

Iridium chloride was added to the slurry solution of HCl and support and gently stirred for 1 hr at room temperature. The slurry was left into water bath at 70 $^{\circ}$C. Then dried at 120 $^{\circ}$C overnight. The catalysts were finally calcinied in air at 300 $^{\circ}$C for 4 hrs and then reduced by flowing hydrogen at (60 cm^3/min) at 500 $^{\circ}$C for 4 hrs. Heating ramps were programmed every 10 $^{\circ}$C /min.

2.2.2 Preparation of Platinum-Tin / Alumina Catalyst

The Pt-Sn/ Al_2O_3 catalyst was prepared by impregnation of the parent catalyst (Pt/Al_2O_3) with tin chloride ($SnCl_2.2H_2O$) in order to reach final concentration of 0.35 wt% Pt and 0.3 wt% of Sn [9]. Tin chloride was dissolved and heated deionized water and heated for 30 min at 70 °C. An amount of 0.2M of HCl solution was added to the support prior the impregnation step in order to assure homogeneous distribution of them. Then added to the catalyst and left for 1 hr unstirred, then gently heated at 70 °C in order to evaporate excess liquid. The catalyst was finally dried at 120 °C for 12 hrs and calcined in air at 500 °C for 4 hrs, final step the catalyst was reduced in flowing hydrogen stream of 60 cm^3/min for 4 hrs at 500 °C.

2.3 Catalysts Performance

All the catalysts were originally in the form of extrudate. Each type was activated inside the reactor, just prior running the tests runs. the reactivation it was 450 and 500 °C for 4 hr respectively in a current of hydrogen at 1 atm pressure and flow ratio of 60 and 80 cm^3/min.

2.4 Heavy Naphtha Units

The catalytic activities studies were carried out in a conventional continuous flow vertical tubular reactor, the dimensions were 20mm internal diameter, 30mm external diameter and 68cm height (reactor volume 214 cm^3). The reactor was charged for each experiment with 50g (catalyst bed 22 cm) of catalyst located in the middle zone, while, the upper and lower zones were filled with glass beads.under different reforming conditions as represented in Fig (1), and (2).

2.5 Operating Procedure

Heavy naphtha pumped under pressure to the reforming unit. Hydrogen mixed with hydrocarbon prior entering the reactor inlet. The mixture was preheated, and then admitted through the catalyst bed. The products were cooled and collected in a separator in order to exhaust the gases to the atmosphere and collect the condensed liquid from bottom of the separator. Products samples were analyzed using gas chromatograph type Shimadzu 2014 GC.

The catalysts bed was tested temperatures (480, 490, 500, and 510 °C), and 6 atm. The weight hourly space velocities were varied at (1, 1.5, and 2 hr^{-1}), and 4:1 hydrogen to hydrocarbon molar ratio. Fresh catalyst was used in each run, therefore deactivation of catalysts will not be need to study in this investigation.

3. Simulation and Mathematical Model

3.1. Introduction

Mathematical modeling in the reforming process has increasingly shown an important tool in petroleum refining industries. It because crucial in developing proper design of new reactor and revamp of existing ones. Modeling can be used to optimize operating conditions, analyze the

effects of process variables, and enhance unit performance. In the present work mathematical models of catalytic reforming reactor can be of complexity which generally depends on description of reactants flow along the reactor, kinetic model of a chemical reaction and mass and energy balance (describe reformate composition.

3.2. Model Description and Assumptions

The main aim of the present study is to analyze the kinetics of reforming process by assessing the effect of reaction time and reaction temperature on the substrate content in the course of process which involves heavy naphtha as raw material. Therefore, three groups of compounds are found which are: Paraffins (normal and iso), naphthenes (N), and Aromatics (A). Then, the physical model for catalytic reforming with mass and energy balance for the element combining kinetic thermodynamic, concentration, and temperature distributions along the reactor length can be calculated.

In developing the model of the catalytic reforming reactor the following assumptions are taken into account.

- Steady state operation and plug flow isothermal operation.
- The pressure is constant throughout the reactor.
- Limiting step was surface reaction.
- Density of reactant and products are constant.
- The temperature and concentration gradients along the radial direction can be neglected and only axial direction are considered.
- All the reforming reactions rates are first order (proved experimentally), all the rate equations are linear pseudo-monomolecular in nature and constant catalyst activity for calculation.

3.3. Kinetics Reaction

According to present work investigation, analysis and monitoring of the heterogeneous reaction (consecutive and parallel) of heavy naphtha catalytic reforming performance schematically represents in Fig (3) as follow

$$\mathbf{P \leftrightarrow N + H_2} \quad \textbf{(1)}$$

$$\mathbf{N \rightarrow A + 3H_2} \quad \textbf{(2)}$$

$$\mathbf{P + H_2 \rightarrow 2G} \quad \textbf{(3)}$$

The kinetic reaction rate is considered to follow simple power law kinetic expression for above reactions [10]:

$$r_1 = k_1 C_P - k_3 C_N P_{H_2} \quad \textbf{(4)}$$

$$r_2 = k_2 C_N \quad \textbf{(5)}$$

$$r_3 = k_4 C_P \quad \textbf{(6)}$$

In general form

$$r_i = k_i C_i^n \quad \textbf{(7)}$$

where

$$k_i = A_\circ EXP\left(\frac{-E_a}{R.T}\right) \text{ [10]} \quad (8)$$

The reaction rate constant k_i confirms the Arrhenius expression:-

$$Lnk_i = LnA_\circ - \frac{E_a}{R.T} \quad (9)$$

The reaction equilibrium constants $K_{eq}= k_1/k_3$. Therefore, equilibrium constant can be calculated by the following thermodynamic relation:

$$K_{eq} = EXP\left(\frac{-\Delta G}{R.T}\right) \text{[11]} \quad (10)$$

the kinetic expression is to be linear (first order with respect to reactants) under the present reactions.

3.4. Kinetic Reaction Model

3.4.1. Mass Balance

To develop a reaction model for an integral reactor, a material balance is made over the cross section of a very short segment of the tubular catalyst bed, as shown in Figure (4):

Then, the resulting equation is:-

$$F_N\Big|_z - F_N\Big|_{z+\Delta z} - V_P \rho(1-Є)(-r_i) = 0 \text{ [12]} \quad (11)$$

As $\Delta z \rightarrow 0$ the differential material balance reduces to:-

$$\frac{dF_n}{dw} = -r_i \quad (12)$$

Where: dw = dv ρ(1-Є)

Now, the reaction rate equations can now be developed for each component in heavy naphtha feed stocks (Paraffins, Naphthenes and Aromatics) as follows:-

$$\frac{dF_P}{dw} = k_3 C_N - (k_4 + k_1) C_P \quad (13)$$

$$\frac{dF_N}{dw} = k_1 C_P - (k_3 + k_2) C_N \quad (14)$$

$$\frac{dF_A}{dw} = k_2 C_N \quad (15)$$

A final modification to the left-hand side of equations (13) to (15) is made by defining a space time variable, θ, as:-

$$\theta = w/f \quad (16)$$

For a constant feed rate, an incremental section of catalyst bed, may expressed as:-

$dw = f.d\theta$ (17)

Substituting equation (17) in above equations (13, 14, and 15) gives:-

$$\frac{dF_P}{d\theta} = k_3 F_N - (k_4 + k_1) F_P \quad (18)$$

$$\frac{dF_N}{d\theta} = k_1 F_P - (k_3 + k_2) F_N \quad (19)$$

$$\frac{dF_A}{d\theta} = k_2 F_N \quad (20)$$

3.4.2. Energy Balance

The equation used to estimate the temperature profile along the reactor is obtained from an energy balance over the differential reactor control volume [13].

$$\mathbf{f.\rho.C_p dT = r_{P\leftrightarrow N}\Delta H_{r,\,P\leftrightarrow N} dV + r_{N\leftrightarrow A}\Delta H_{r,\,N\leftrightarrow A} dV + r_{P\rightarrow G}\Delta H_{r,\,P\rightarrow G} dv} \quad (21)$$

Substituting equations (17) in to above equation yield:-

$$\frac{dT}{d\theta} = \frac{1}{\rho C_P}\begin{pmatrix} r_{P\leftrightarrow N}\Delta H_{r,P\leftrightarrow N} \\ + r_{N\rightarrow A}\Delta H_{r,N\rightarrow A} \\ + r_{P\rightarrow G}\Delta H_{P\rightarrow G} \end{pmatrix} \quad (22)$$

The above differential equation is taken to be as first order and this is improved experimentally as:-

$$-r_i = k_i C_i^n \quad \mathbf{(7)}$$

Taking Ln for both side of above equation yield:

$$Ln(-r_i) = Lnk_i + nLnC_i \quad \mathbf{(23)}$$

By plotting Ln ($-r_i$) vs. LnC_i, then, the behaviors of first order must be straight line (tan 45° = 1) as shown in Fig (5) and (6) for different reaction and different catalyst. These two figures are just samples for some selected types of both catalysts.

3.5. Process Model

The physical model for catalytic reforming axial flow reactor is shown in Fig (4). The following ordinary differential equations for mass and energy balance were integrated through each reactor bed to describe reformate composition and temperature profile along the length of the reactor. The system is numerically solved by method of finite difference approach with explicit solution of all the differential equation in the mathematical model. And a schematic step of reactor models has shown in figure (7).

For Mass balance:

$$\frac{dY_i}{dZ} = \sum_{Ii=1}^{m} \frac{MW}{z.WHSV}\left(-r_i\right)^{[14]} \tag{24}$$

If substitute's heavy naphtha components (Paraffin, Naphthene, and Aromatic) then equation (24) become:

$$\frac{dY_P}{dZ} = \frac{MW}{z.WHSV}\left[r_{N\to P} - \left(r_{P\to N} + r_{P\to G}\right)\right] \tag{25}$$

$$\frac{dY_N}{dZ} = \frac{MW}{z.WHSV}\left[r_{P\to N} - \left(r_{N\to P} + r_{N\to A}\right)\right] \tag{26}$$

$$\frac{dY_A}{dZ} = \frac{MW}{z.WHSV}\left(r_{N\to A}\right) \tag{27}$$

For energy balance:

$$\frac{dT}{dZ} = S\frac{\sum_{I=1}^{m} r_i\left(-\Delta H r_i\right)}{\sum_{I=1}^{m} f_i C_{P_i}}\ [14] \tag{28}$$

$$\frac{dT}{dZ} = \frac{S}{\sum_{I=1}^{m} f_i C_{P_i}}\begin{bmatrix} r_{P\to N}\left(-\Delta H_{r,P\to N}\right) \\ + r_{N\to A}\left(-\Delta H_{r,N\to A}\right) \\ + r_{N\to P}\left(-\Delta H_{r,N\to P}\right) \\ + r_{P\to G}\left(-\Delta H_{P\to G}\right) \end{bmatrix} \tag{29}$$

$$\Delta H^{\circ}_{r,T} = \Delta H^{\circ}_{r,298} + \int_{298}^{T} \Delta C_P dT\ ^{[15]} \tag{30}$$

The results of heat reactions estimations are represented in Table (3).

3.6. Estimation of Reaction Kinetic Parameters

The apparent activation energy $\left(E_a\right)$ is established from Arrhenius equation that satisfies the relationships between rate constant and reaction temperature as given in equations (7, 8, and 9). From plot of $Ln(k)$ vs. (1/T) up shown in Figs (8) and (9). The values of activation energy were calculated from the slope represented by ($-E_a/R.T$) and the intercept represented by $Ln\left(A_{\circ}\right)$ let us to determine the value of pre-exponential factor. Results of each catalysts type are listed in Table (3).

4. Results and Discussions

4.1 Effect of Temperature

Result of Figs (10) and (11) show that the concentration of light components (n-P_5 and n-P_6) is increased with an increase in the reaction temperature. At the same figure illustrates that, the heavier components concentration % decrease as reaction temperatures increases, which is

attributed to the dehydrocyclization reaction which is favored at higher reaction temperature and higher molecular weight of carbon number [16].

The results that are shown in Figs (12) and (13) shown higher iso-P_6 increases with temperature increase. Where as iso-P_7 content increases as reaction temperature increases and then decreases at higher temperature. From the same figure it can be seen that, the heavier paraffin's contents decreases with temperature increase.

Figures (14) and (15) shows that naphthenes mole % decreases as reaction temperature increases, since the conversion of naphthenes to aromatics is the primary naphthene reaction and is regarded the most favorable amongst with all other reactions in catalytic reforming. It is important to mention here that the reactivity of dehydrogenation reactions increases with an increase in naphthenes carbon number [17].

Figures (16) and (17), shows that the mole percentage of aromatics components increases as the reaction temperatures increased. This behavior can be explained on the basis of that the dehydrogenation of naphthenes and dehydrocyclization of paraffin's became faster with an increase in temperature and carbon number.

The comparison between the performance of the two types of catalysts (Pt-Sn/ γ-Al_2O_3, Pt-Ir/ γ-Al_2O_3) shows that the first type is better than the second one because the addition of tin has enhance the selectivity of isomerization, and increases the aromatization reaction [18]. It is clear that the aromatic mole% produced from the reaction is about 30.4 mole % at 510 °C and 26.56 mole% for the second type of catalyst under the same condition. Then, it can be concluded that the use of tin with platinum will lead to improvement of the dehydrogenation and dehydrocyclization reactions rather than iridium.

4.2. Effect of Weight Hour Space Velocity

The influence of weight hourly space velocity was studied at (1, 1.5, and 2 hr^{-1}), and temperature of (510 ˚C). Which gave the highest aromatics yield.

Figures (18) and (19) have clearly illustrated that the mole% of light component (n-P_5 and n-P_6) decreases as WHSV increases; this behavior is due to the slow rate of hydrocracking reaction. Therefore, the increase in WHSV causes a decrease in the residence time, which offers plenty of contact time of feedstock with the catalyst inside reactor, which latter lead to an effective conversion of n-paraffins [19]. It can also observe that the heavier paraffins reactivity decreases as WHSV increases.

Figures (20) and (21) show that the iso-Paraffins components decrease with increasing of WHSV, but this decrease is less than the decreases in n-paraffin. Such conclusion is attributed to

the fact that selectivity of paraffin's isomerization reactions at typical reforming operating condition is relatively insignificant to space velocity [20].

Figures (22) and (23) show same general trend of decreasing of naphthenes components conversion to aromatics via dehydrogenation reaction (mole % increase, means reactivity decrease) with increasing WHSV. The slights decrease in this trend is directly to the dehydrogenation reaction which is the fastest reaction among all heavy naphtha reforming reactions [13].

From Figures (24) and (25) it is observed that, increasing of WHSV will lead to a decrease in the aromatics yield. It is important to mention here that the aromatics components are produced from dehydrogenation of naphthenes which is not affected too much with WHSV and from dehydrocyclization reaction of Paraffins (n and iso), where, it is the slowest reaction and is affected by the increasing of WHSV and that attributed to the low contact time with the catalyst [21].

4.3. Simulation Results of Mathematical Model

Figures (26) and (27) show the concentration profiles for reactants (Paraffins and Naphthenes) and products (Aromatics and Gases) for all catalysts types used in the present work at 480 ˚C and WHSV of $1hr^{-1}$ as an example.

Figures (28) and (29) show the comparison between the experimental and predicted conversion of Paraffins and Naphthenes and Aromatics for all catalysts types. Tables (4) represent the comparison between theoretical and experimental data.

The predicted temperature profiles using Pt-Sn / γ-Al_2O_3 along bed length at temperatures 480, and 490 ˚C can be seen in Figures (30) and (31). The results from these figures give the trend of temperature profile which decreases along the catalyst bed length (distance), for all temperature ranges. This trend agrees with the published results for heavy naphtha catalytic reforming process. Many researches indicate that the temperature decreases along the catalyst bed, because reforming process reactions are, overall, endothermic. For this reason, commercial catalytic reformers are designed with multiple reactors and with heaters between the reactors to maintain reaction temperature at operatable levels [14, 16, and 21].

Conclusion

The addition of tin (Sn) and iridium (Ir) to Pt/ γ-Al_2O_3 as bi-metal (Pt-Sn/ Al_2O_3, and Pt-Ir/Al_2O_3) improves the conversion of heavy naphtha reactants (Paraffins and Naphthenes). On the other hand, the selectivity of catalysts toward aromatization reactions especially light aromatics (A_6, and A_7) is increased.

The conversion of heavy naphtha reactants (Paraffins and Naphthenes) increases with increasing of reaction temperature in the range (480 – 510 °C), for the catalyst (Pt-Sn/ Al_2O_3) conversion % increasing from (14.75 % - 24.24 %) for (Paraffins) and (60 % - 71.9 %) for (Naphthenes), while for (Pt-Ir/ Al_2O_3) catalyst conversion % increasing from (8.57 % - 16.7 %) for (Paraffins) and (50 % - 63.15 %) for (Naphthenes) and decreases with increasing of weight hour space velocity above (1 hr^{-1}). The yield of the desired products (Aromatics) increases with increasing of reaction temperature in the range (480 – 510 °C) for (Pt-Sn/ Al_2O_3) catalyst increasing from (28.27 % - 33.67 %), while for (Pt-Ir/ Al_2O_3) catalyst increasing from (24.51% - 29.41%) and decreases with increasing of weight hour space velocity.

The derived model and simulation agrees with the experimental work results according to the suggested scheme of reactions network for heavy naphtha reforming. And the comparison of model results with experimental results shows a deviation range of (0.36 % to 15.51 %).

References

1- Silvana A.D., Carlos R.V., Florence E., Catherine E., Patrice M., Carlos L.P. 2008," Naphtha Reforming Pt-Re-Ge/ γ-Al_2O_3 Catalysts Prepared by Catalytic Reduction (Influence of the pH of the Ge Addition Step) ", J. Catal Today, vol 133-135, p 13-19,.

2- Viviana B., Marieme B., Vanina A.M., Catherine E., Florence E., Carlos R.V., Patrice M., Carlos L.P. 2007," Preparation of Tri-metallic Pt-Re-Ge/ Al_2O_3 and Pt-Re-Sn/ Al_2O_3 Naphtha Reforming Catalysts by Surface Redox Reaction ", J. Appl. Catal A: vol 319, p 210-217.

3- Meyers R.A. 2006," HandBook of Petroleum Refining Processing", McGraw Hill, 3rd Edition, Copyrighted Material, USA.

4- Pieck C.L., Carlos R.V., Parera M.,Gustavo N.G., Luciano R.S., Luciene S.C., and Maria C.R. 2005.," Metal Dispersion and Catalytic Activity of Trimetallic Pt-Re-Sn/ Al_2O_3 Naphtha Reforming Catalysts ",J.Catal. Today, vol 107-108, 30 0ct, p 637.

5- Caravalho L.S., Piek C.L., Rangel M.C., Figoli N.S., Grau J.M., Reyes P., Parera J.m. 2004.," Trimetallic Naphtha Reforming Catalysts. I. Properties of the Metal Function and Influence of the Order of Addition of the Metal Precursors on Pt-Re-Sn/ γ-Al_2O_3-Cl ", J. Appl. Catal A: vol 269, p 91-103.

6- Weifeng H., Hongye S., Yongyou H., and Tiom C.," Modeling, Simulation and Optimization of a whole Industrial Catalytic Naphtha Reforming Process on Aspen plus Platform", Chinese, J.Chem. Eng, vol 14, No 5, p 584, 2006.

7- Juarez J.A, Macias E.V. 2000," On the Kinetics of Catalytic Reforming with the Use of Various Raw Material" J. Energy and Fuel, vol 14, p1032-1037.

8- Florence E., Christelle C., Patrice M. 2005," Catalytic Properties in n-heptane Reforming of Pt-Sn and Pt-Ir-Sn/ γ-AL_2O_3 Catalysts Prepared by Surface Redox Reaction", J. Appl. Catalysis A: vol 295, p 157-169.

9- González M.P., Iñarra B., Guil J.M., Gutiérrez M.A. 2005," Development of an Industrial Characterisation Method for Naphtha Reforming Bimetallic Pt-Sn/ γ-Al_2O_3 Catalysts through n-heptane Reforming Test Reaction ", J. Catal. Today, vol 107-108, p 685-692.

10- Fogler S.C. 1997," Element of Chemical Reaction Engineering", 2nd Edition, Prentice-Hall of India Private Limited,.

11- Yong H., Hongy S., Jian C. 2003," Modeling, Simulation and Optimization of Commercial Naphtha Catalytic Reforming Process ", Proceeding of the 42nd IEEE Conf, USA, (Dec), p 6206.

12- Aguilar R.E., Ancheyta J.J. 1994," New Process Model Proves Accurate in Tests on Catalytic Reformer ", Oil Gas J, vol 25, p 80-83.

13- Gates B.C., Katzer J.R., Schuilt G.C.A. 1979," Chemistry of Catalytic Processes", McGraw-Hill book Co. New York, p 184.

14- Villafertre E., Jorge A.J. 2002," Kinetic and Reactor Modeling of Naphtha Reforming Process", J. Petroleum and Coal, vol 44, 1-2, p 63-66.

15- Lu H. 1982," Manual of Petrochemical Industry Fundamental Data", Chemical Industry Press, Beijing, China,.

16- Seif Mohaddecy S.R., Zahedi S., Sadighi S., Bonyad H. 2006," Reactor Modeling and Simulation of Catalytic Reforming Process ", J. Petroleum and Coal, vol 48, No3, p 28-35.

17- Vanina A.M., Javier M.G., Carlos R.V., Juan C.Y., José M.P., Carlos C.Y. 2005," Role of Sn in Pt-Re-Sn/AL_2O_3-Cl Catalysts for Naphtha Reforming ", J. Catal Today, vol 107-108, p 643-650.

18- Bednarova L., Lyman C.E., Rytter E., Holmen A. 2002, J. Catal, vol 211, p 335.

19- Mohammed A.A., Hussein K.H. 2004," Catalytic Aromatization of Naphtha Using Different Catalysts", Iraq. J. Chem. and Petr Eng, vol 5, (Dec), p 13.

20- Jenkins J.H., Stephens T.W. 1980," Kinetics of Catalytic Reforming", J. Hyd. Proc, Nov, p 163-167.

21- Ali S.A., Siddiqui M.A. 2006," Parametric Study of Catalytic Reforming Process", J. React .Kinet. Catal. Litt, vol 87, (No 1), p 199-206.

Nomenclature

Symbol	Definition	Units	Symbol	Definition	Units
A	Aromatics	(-)	K_{eq}	Reaction equilibrium constant	(-)
$A_\circ$	Pre-exponential factor	(-)	LHSV	Liquid hour space velocity	hr^{-1}
A_i	Aromatics(6,7,8,9) carbon atom	(-)	MW	Molecular weight	g/gmole
C_N	Naphthenes concentration	$mole/cm^3$	N_i	Naphthene (5,6,7,8,9) carbon atom	(-)
C_n.	Initial concentration of species n	$mole/cm^3$	n-P_i	Paraffine(5,6,7,8,910)carbon atom	(-)
C_n	Concentration of species n	$mole/cm^3$	P	Paraffin	(-)
Cp	Specific heat	J/mole.°C	P_a	Total pressure	atm
Ea	Activation energy	kJ/mole	R	Gas constant	J/mole.K
F_A.	Molar flow rate of component A	mole/hr	r_i	Reaction rate of species i	mole/gcat. hr
F_n.	Initial molar flow rate of species n	mole/hr	r_1	Reaction rate for paraffin's dehydrocyclization reaction	mole/gcat. hr
F_n	Molar flow rate of species n	mole/hr	r_2	Reaction rate for naphthene's dehydrogenation reaction	mole/gcat. hr
f	Weight flow rate	g / hr	r_3	Reaction rate for paraffin's hydrocracking reaction	mole/gcat. hr
G	Gases	(-)	T	Reaction temperature	°C
GC	Gas chromatography	(-)	$T^{\bullet}$	Initial temperature	°C
H_2	Hydrogen	(-)	V	Volume of gas adsorbed at the equilibrium pressure	cm^3
ΔH°_r	Heat of i th reaction	J/ mole	$V_\circ$	Volume of gas adsorbed by the sample	cm^3
H_2/H.C	Hydrogen to hydrocarbon mole ratio	(-)	V_C	Volume of catalyst	cm^3
iso-P	Iso-paraffins	(-)	W	Weight of catalyst	kg
k	Reaction rate constant	hr^{-1}	WHSV	Weight hour space velocity	hr^{-1}
k_1	Rate constant for paraffin's cyclization	hr^{-1}	Y_i	Molar composition of species i (A, N, and P)	(-)
k_2	Rate constant for naphthenes dehydrogenation	hr^{-1}	zt	Length of reactor	cm
k_3	Rate constant for naphthenes hydroisomerization	hr^{-1}	Δz	Integration step for the reactor length	(-)
k_4	Rate constant for paraffins hydrocracking	hr^{-1}	ϵ	Porosity of catalyst bed	cm^3/cm^3

Table (1): The properties of heavy naphtha (Al-Dura refinery)

Property	Unit	Data
Specific Gravity at 15.6 ˚C	-	0.733
API	-	61.7
Distillation		
I.B.P	°C	60
10 vol % distilled	°C	88
20 vol% distilled	°C	94
30 vol% distilled	°C	106
40 vol% distilled	°C	110
50 vol % distilled	°C	117
60 vol% distilled	°C	124
70 v0l% distilled	°C	132
80 vol% distilled	°C	140
90 vol % distilled	°C	147
F.B.P	°C	178
Total distillate	vol%	98.5
Total recovery	vol%	99.5
Residue	vol%	1
Loss	vol%	0.5
Sulfur Content	ppm	3
Mwt.	g/gmol	108
Total Paraffin	vol %	60
Total naphthene and aromatic	vol %	40

Table (2): Physical and chemical properties of commercial and prepared catalysts.

	Commercial $Pt/\gamma\text{-}Al_2O_3$	Commercial $Pt\text{-}Re/\gamma\text{-}Al_2O_3$	Prepared $Pt\text{-}Sn/\gamma\text{-}Al_2O_3$	Prepared $Pt\text{-}Ir/\gamma\text{-}Al_2O_3$
Pt , wt %	0.35	0.3	0.35	0.5
Re, wt %	-	0.3	-	-
Sn ,wt %	-	-	0.3	-
Ir , wt %	-	-	-	0.1
Form	Extrudate	Extrudate	Extrudate	Extrudate
Surface Area m^2 / g	220	220	205.4	219.9
Pore Volume cm^3 / g	0..57	0.6	0.68	0.61
Bulk Density g / cm^3	0.66	0.69	0.624	0.67

Table (3): Results of analysis of heat of reaction

ΔH°_r (J/mole H_2)				
Reaction	**480 °C**	**490 °C**	**500 °C**	**510 °C**
$N + H_2 \rightarrow P$	**-54393.3**	**-54238.5**	**-53903.7**	**-53648.5**
$N \rightarrow A + 3H_2$	**73119.9**	**73207.8**	**73291.5**	**73361.2**
$P + (n-3/3)\ H_2 \rightarrow n/15(C_1-C_5)$	**-52623.1**	**-52837.6**	**-53079.3**	**-53309.7**

Table (4) :Activation energy values and pre-exponential factor for bi-metal catalysts.

Reaction	**Ea/R**	**Ea kcal/mol**	**A◦**
$Pt-Sn/\gamma-Al_2O_3$			
$P \rightarrow N + H_2$	**15084**	**125.40**	**$7.927*10^8$**
$N + H_2 \rightarrow P$	**10674**	**88.74**	**$6.733*10^5$**
$N \rightarrow A + 3H_2$	**9822.2**	**81.63**	**$7.997*10^5$**
$P + H_2 \rightarrow 2G$	**11905**	**98.95**	**$5.803*10^6$**
$Pt-Ir/\gamma-Al_2O_3$			
$P \rightarrow N + H_2$	**15802**	**131.39**	**$1.173*10^9$**
$N + H_2 \rightarrow P$	**11400**	**94.77**	**$1.005*10^6$**
$N \rightarrow A + 3H_2$	**9841.3**	**81.80**	**$1.561*10^6$**
$P + H_2 \rightarrow 2G$	**13859**	**115.19**	**$3.616*10^6$**

Table (5) comparison between theoretical and experimental conversions for bi-metal catalyst at constant WHSV ($1hr^{-1}$) for different reaction temperatures

Condition	**Components**	**$Pt-Sn/\gamma-Al_2O_3$**		**Relative deviation %**	**$Pt-Ir/\gamma-Al_2O_3$**		**Relative deviation %**
		Exp. Conv %	**Theo. Conv%**		**Exp. Conv%**	**Theo. Conv %**	
480 °C	**Paraffins**	**6.03**	**6.72**	**10.26**	**3.71**	**4.34**	**14.51**
490 °C	**Paraffins**	**7.90**	**8.40**	**6**	**5.52**	**5.54**	**0.36**
500 °C	**Paraffins**	**9.66**	**10.40**	**7.11**	**7.18**	**7.02**	**2.28**
510 °C	**Paraffins**	**11.84**	**12.78**	**7.35**	**8.65**	**8.82**	**1.93**
480 °C	**Naphthenes**	**50.16**	**52.51**	**4.47**	**44.40**	**47.29**	**6.11**
490 °C	**Naphthenes**	**51.10**	**56.84**	**10.10**	**48.17**	**51.85**	**7.10**
500 °C	**Naphthenes**	**54.75**	**60.84**	**10**	**50.81**	**56.21**	**9.6**
510 °C	**Naphthenes**	**55.12**	**64.40**	**14.41**	**51.94**	**60.29**	**13.85**
480 °C	**Aromatics**	**1.734**	**1.814**	**4.41**	**1.504**	**1.691**	**11.1**
490 °C	**Aromatics**	**1.797**	**1.911**	**5.96**	**1.622**	**1.778**	**8.77**
500 °C	**Aromatics**	**1.945**	**2.013**	**3.38**	**1.729**	**1.869**	**7.50**
510 °C	**Aromatics**	**2.065**	**2.121**	**2.64**	**1.804**	**1.964**	**8.17**

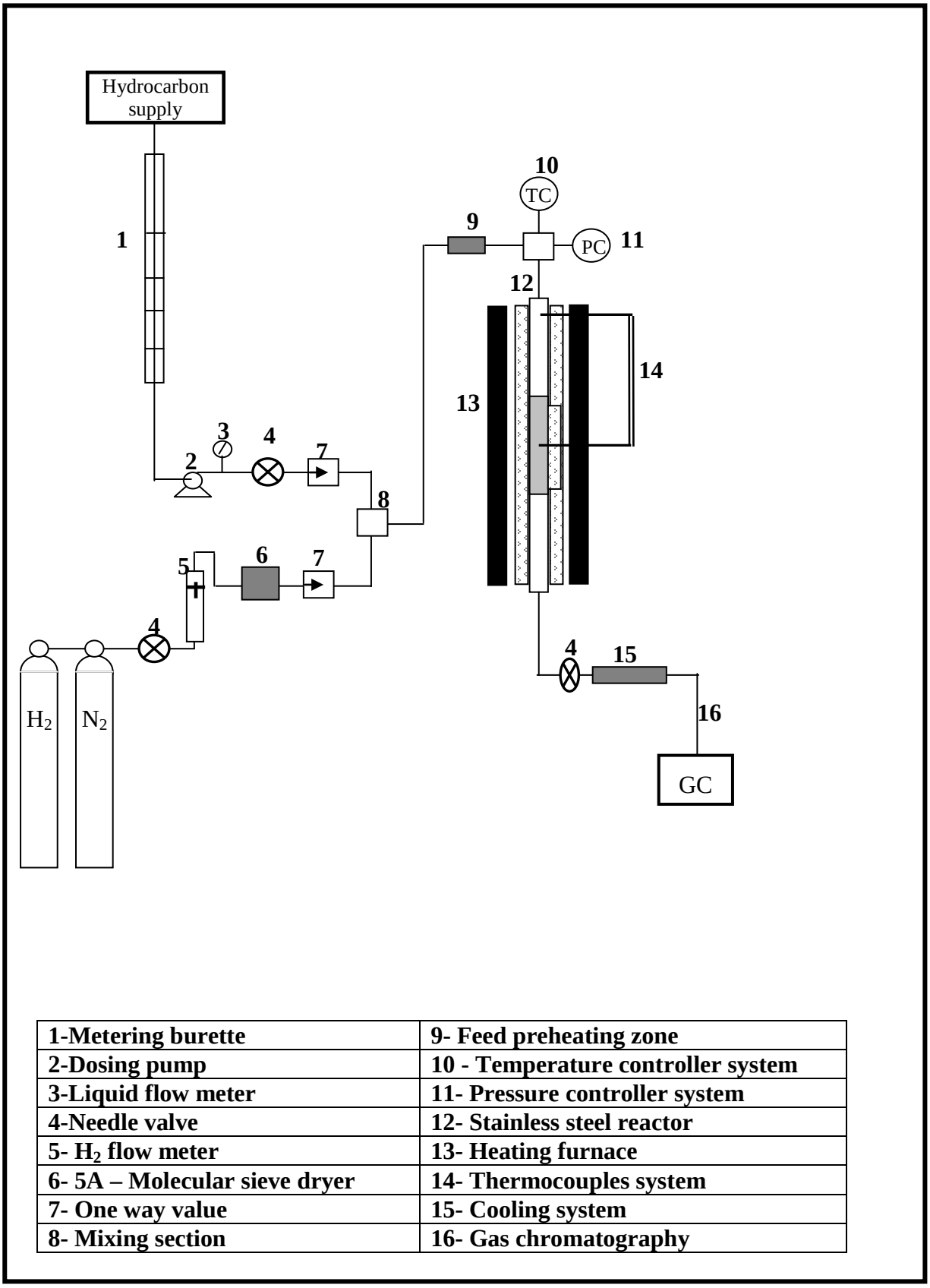

1-Metering burette	**9- Feed preheating zone**
2-Dosing pump	**10 - Temperature controller system**
3-Liquid flow meter	**11- Pressure controller system**
4-Needle valve	**12- Stainless steel reactor**
5- H_2 flow meter	**13- Heating furnace**
6- 5A – Molecular sieve dryer	**14- Thermocouples system**
7- One way value	**15- Cooling system**
8- Mixing section	**16- Gas chromatography**

Figure (1): Schematic diagram of the experimental apparatus of naphtha catalytic reforming unit.

Figure (2): Gas chromatographic analysis.

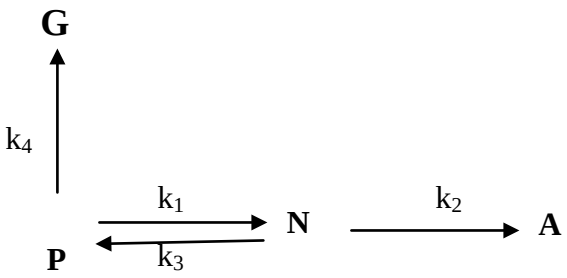

Figure (3) The suggested reactions network of heavy naphtha reforming of the present work.

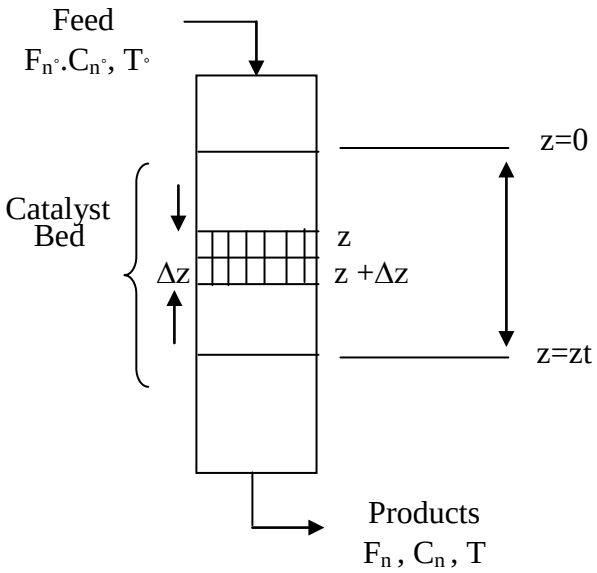

Figure (4) Segment of tubular reactor

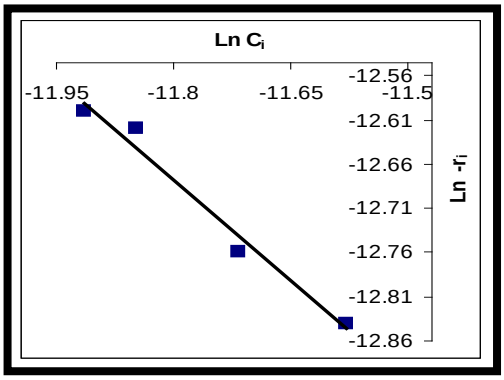

Figure (5) Plot for $N+H_2 \rightarrow P$ for Pt-Ir catalyst at 1.5 hr^{-1}

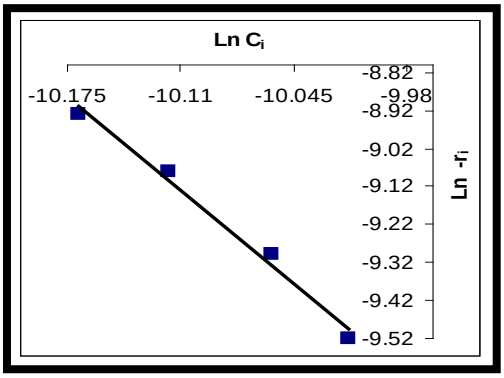

Figure (6) Plot for $P \rightarrow N+H_2$ for Pt-Sn catalyst at 1.5 hr^{-1}

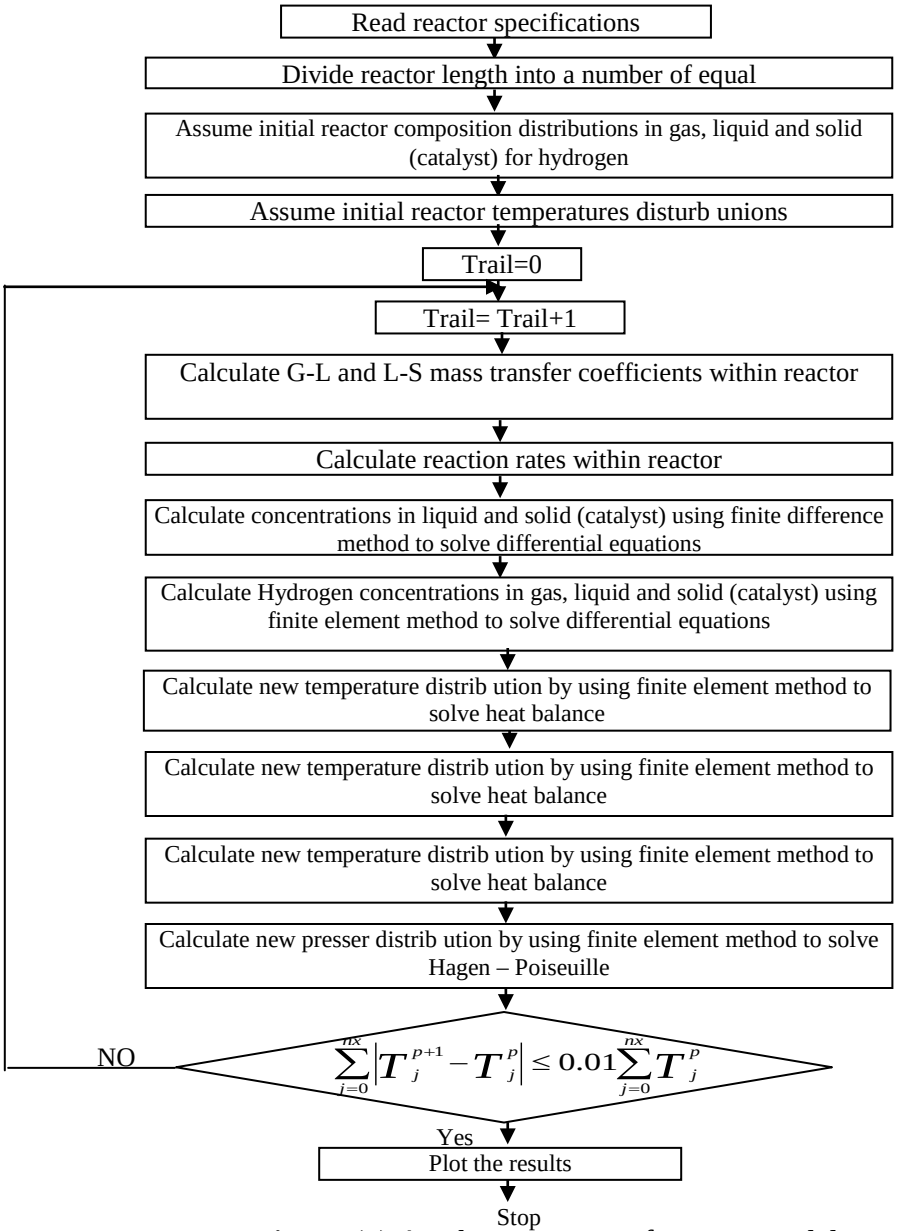

Figure (7) A-schematic step of reactor models.

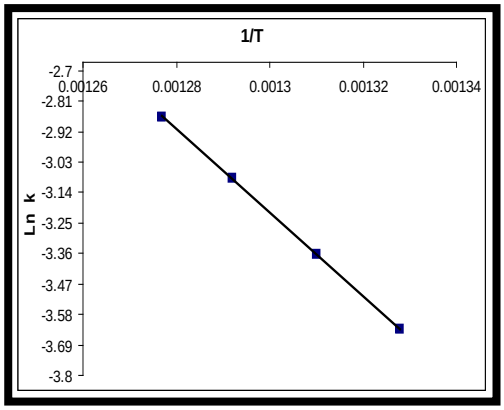

Figure (8) Arrhenius plot for the reaction P → N + H_2 for Pt-Sn/γ-Al_2O_3.

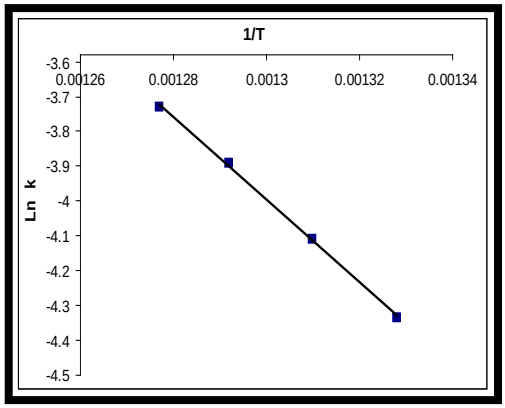

Figure (9) Arrhenius plot for the reaction P + H_2 → 2G for Pt-Sn/γ-Al_2O_3.

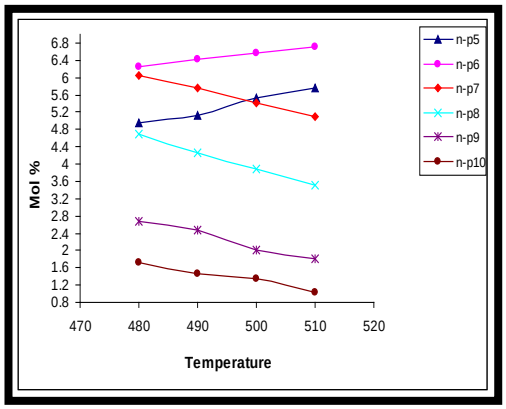

Figure (10) Effect of temperature on the mole % of n-Paraffins components at WHSV of (1 hr^{-1}) for (Pt-Sn / γ-Al_2O_3) catalyst.

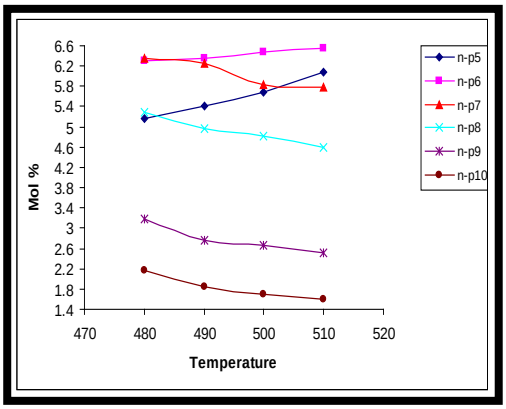

Figure (11) Effect of temperature on the mole % of n-Paraffins components at WHSV of (1 hr^{-1}) for (Pt-Ir / γ-Al_2O_3) catalyst.

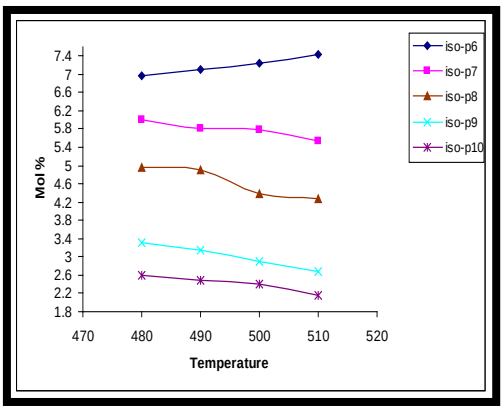

Figure (12) Effect of temperature on the mole % of iso-Paraffins components at WHSV of (1 hr^{-1}) for (Pt-Sn / γ-Al_2O_3) catalyst.

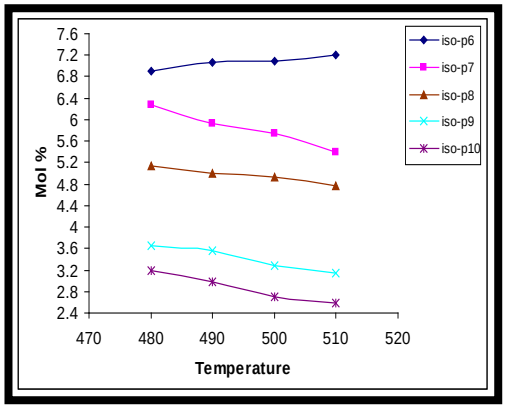

Figure (13) Effect of temperature on the mole % of iso-Paraffins components at WHSV of (1 hr^{-1}) for (Pt-Ir / γ-Al_2O_3) catalyst.

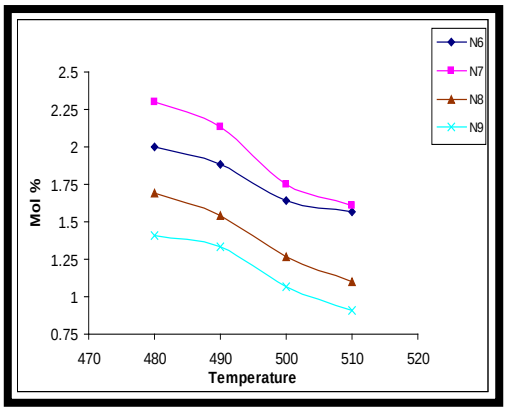

Figure (14) Effect of temperature on the mole % of naphthenes components at WHSV of (1 hr^{-1}) for (Pt-Sn / γ-Al_2O_3) catalyst.

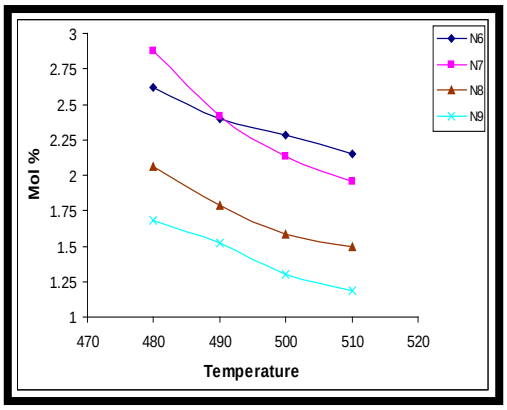

Figure (15) Effect of temperature on the mole % of naphthenes components at WHSV of (1 hr^{-1}) for (Pt-Ir / γ-Al_2O_3) catalyst.

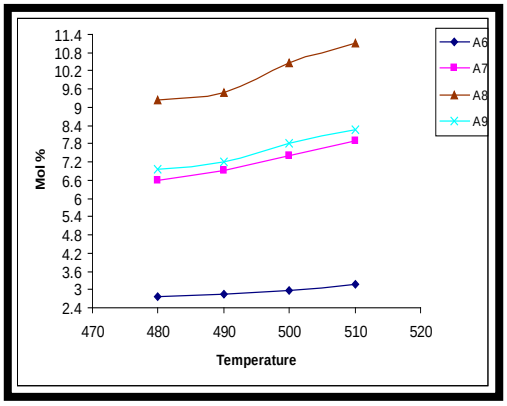

Figure (16) Effect of temperature on the mole % of aromatics components at WHSV of (1 hr^{-1}) for (Pt-Sn / γ-Al_2O_3) catalyst.

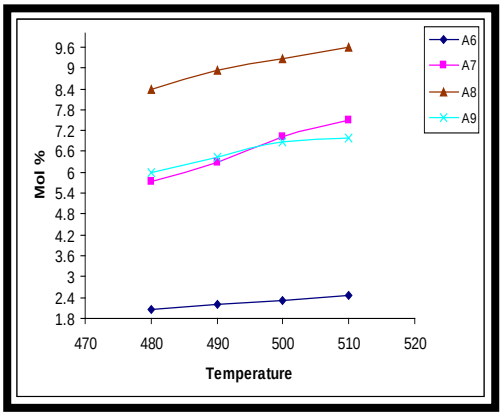

Figure (17) Effect of temperature on the mole % of aromatics components at WHSV of (1 hr^{-1}) for (Pt-Ir / γ-Al_2O_3) catalyst

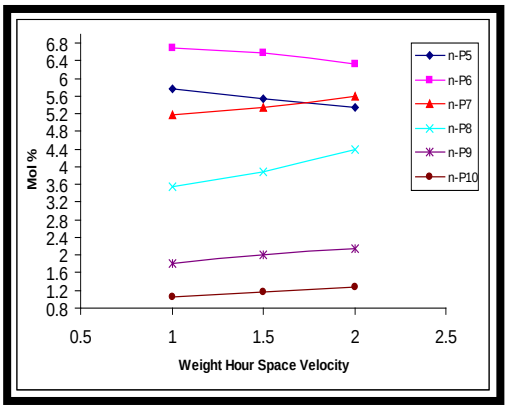

Figure (18) Effect of weight hour space velocity on the mole % of n-Paraffins components at 510 °C for (Pt-Sn / γ-Al_2O_3) catalyst.

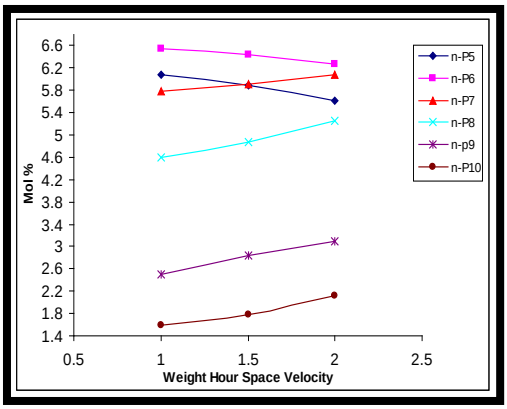

Figure (19) Effect of weight hour space velocity on the mole % of n-Paraffins components at 510 °C for (Pt-Ir / γ-Al_2O_3) catalyst.

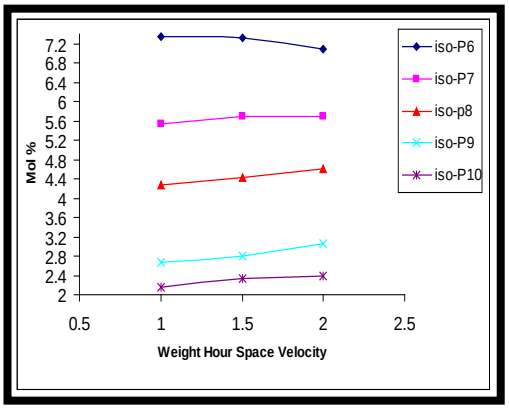

Figure (20) Effect of weight hour space velocity on the mole % of iso-Paraffins components at 510 °C for (Pt-Ir / γ-Al_2O_3) catalyst.

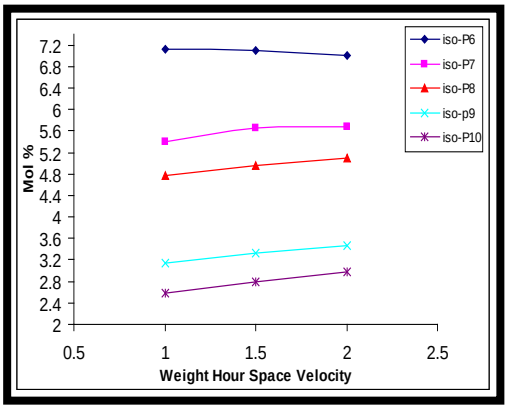

Figure (21) Effect of weight hour space velocity on the mole % of iso-Paraffins components at 510 °C for (Pt-Sn / γ-Al_2O_3) catalyst.

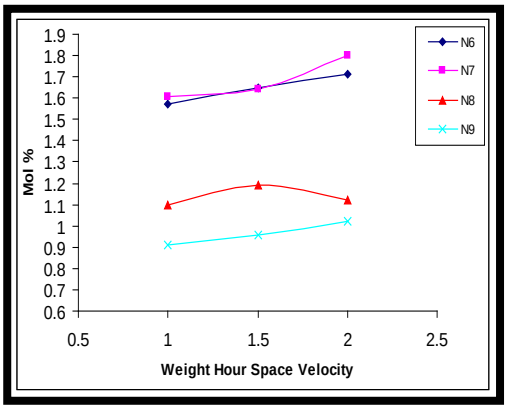

Figure (22) Effect of weight hour space velocity on the mole % of naphthenes components at 510 °C for (Pt-Ir / γ-Al_2O_3) catalyst.

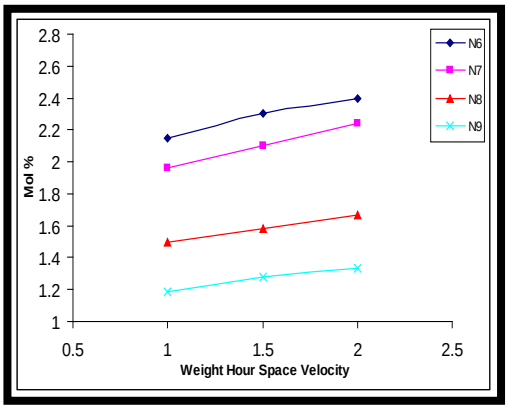

Figure (23) Effect of weight hour space velocity on the mole % of naphthenes components at 510 °C for (Pt-Sn / γ-Al_2O_3) catalyst.

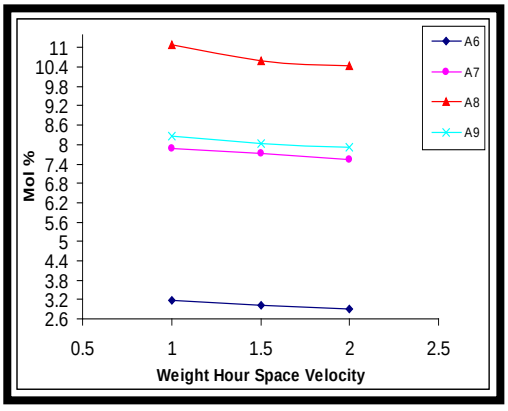

Figure (24) Effect of weight hour space velocity on the mole % of aromatics components at 510 °C for (Pt-Sn / γ-Al_2O_3) catalyst.

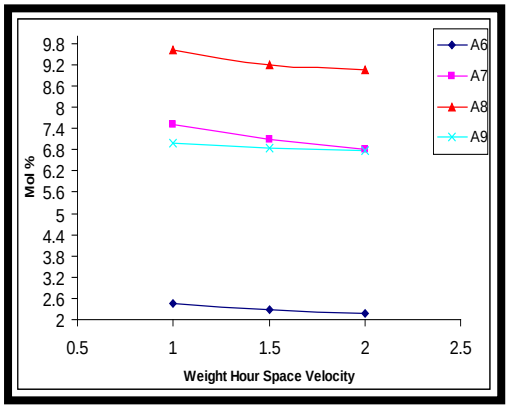

Figure (25) Effect of weight hour space velocity on the mole % of aromatics components at 510 °C for (Pt-Ir / γ-Al_2O_3) catalyst.

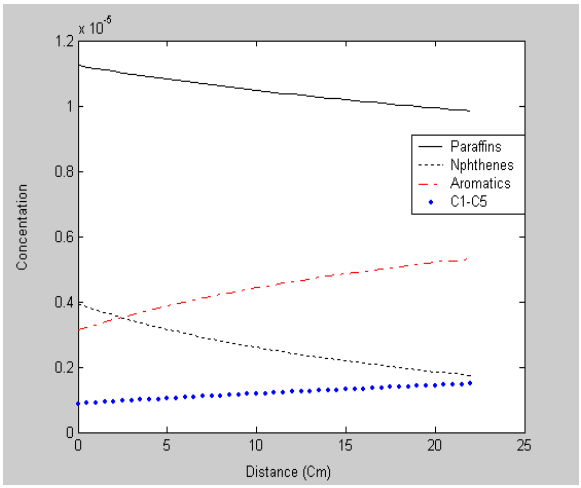

Figure (26) Concentration profiles for (Paraffins, Naphthenes, Aromatics, and gases) at 480 °C and (1 hr^{-1}) for (Pt-Sn / γ-Al_2O_3) catalyst.

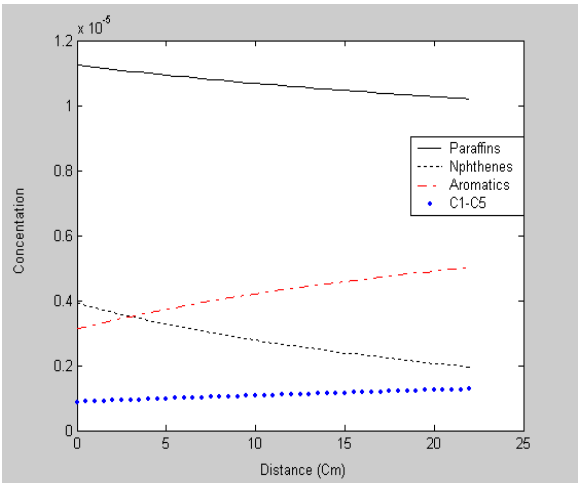

Figure (27) Concentration profiles for (Paraffins, Naphthenes, Aromatics, and gases) at 480 °C and (1 hr^{-1}) for (Pt-Ir / γ-Al_2O_3) catalyst.

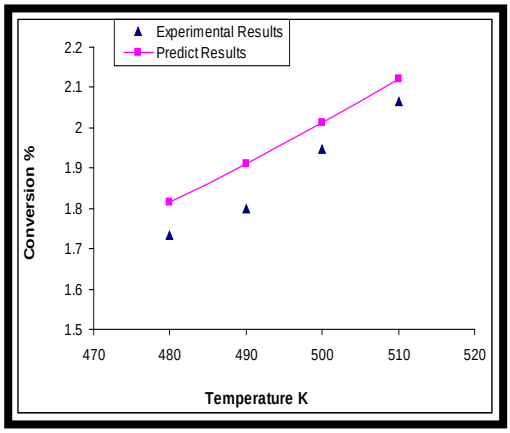

Figure (28) The comparison between the experimental and predicted aromatics conversion at WHSV of (1hr^{-1}) for (Pt-Sn / γ-Al_2O_3) catalyst.

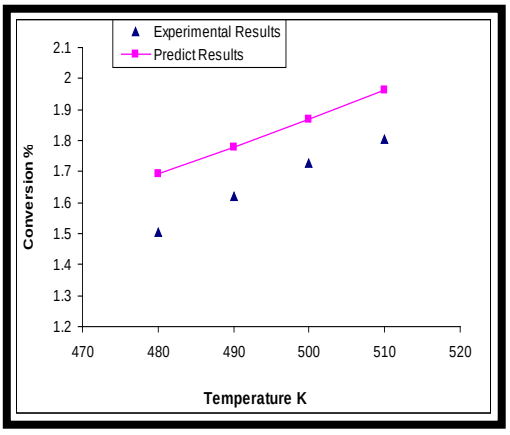

Figure (29) The comparison between the experimental and predicted aromatics conversion at WHSV of (1hr^{-1}) for (Pt-Ir / γ-Al_2O_3) catalyst.

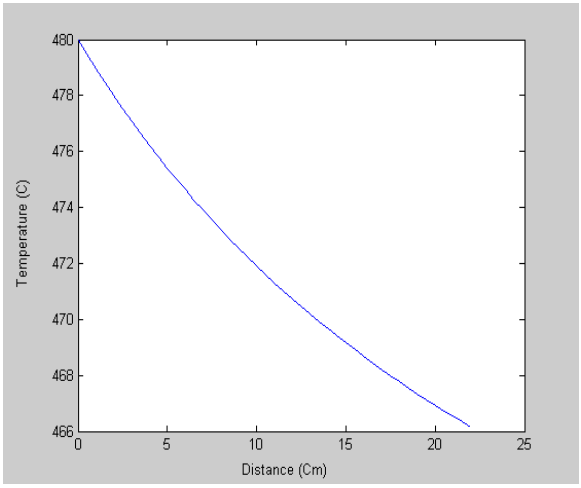

Figure (30) Simulation of temperature profile for (Pt-Sn / γ-Al_2O_3) catalyst at 480 °C and (1hr^{-1}).

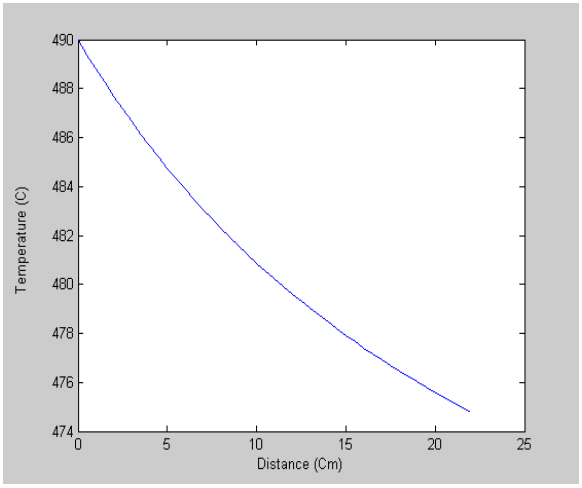

Figure (31) Simulation of temperature profile for (Pt-Sn / γ-Al_2O_3) catalyst at 490 °C and (1hr^{-1}).

دراسة محاكاة تفاعلات التهذيب لمادة النفثا الثقيلة باستخدام عوامل مساعدة ثنائية المعدن $Pt\text{-}Sn/AL_2O_3$ and $Pt\text{-}Ir/AL_2O_3$

خالد عجمي سكر، شهرزاد رفعت روؤف، رمزي صيهود حميد

أ.م.دزخالد عجمي سكر,Khalid_ajmee@yahoo.co قسم تكنولوجيا النفط / الجامعة التكنولوجية / العراق

أ.م.د. شهرزاد رفعت روؤف ، srraouf@yahoo.uk.co قسم الهندسة الكيمياوية / الجامعة التكنولوجية / العراق

د. رمزي صيهود حميد , ramze_eng@yahoo.co قسم تكنولوجيا النفط / الجامعة التكنولوجية / العراق

تـضمن البحث اعداد دراســة شاملة عمليــة ونظريــة للعوامل المساعدة ثنائية المعدن المحملة على الالومينا($Pt\text{-}Sn/AL_2O_3$) المستخدمة في عملية التهذيب باستخدام مـادة النفثـا الثقيـلة (العراقيـة) كمادة اولية للعملية .من اجل دراسة امكانية زيادة كفاءة العملية وتحسين أنتقائية العوامل المساعدة تم خلال البحث دراســة التفاعـلات الرئيسية التي تحدث في عملية التهذيب وهي (تفاعـلات ازالة الهيدروجين، تفاعلات تكوين المركبات الحلقية وكذلك تفاعـلات التكسير الحراري) بوجود الهيدروجين. تم دراسة اداء نوعين من العوامل المساعدة الثنائية المعدن حسب الضروف التشغيلية التالية : السرعة الفراغية للغاز(2-1 ساعة$^{-1}$) ، درجة حرارة التفاعل تتراوح بين (510-480 م°). أثبتت النتائج العملية ان نسبة التحول لمادة النفثا الثقيلة (المواد البرافينية والمواد النفثينية) تزداد مع زيادة درجة حرارة التفاعل وتقل مع زيادة السرعة الفراغية. كذلك لوحظ ان الانتاجية (yield) للمواد العطرية والمركبات الخفيفة تزداد لجميع انواع العوامل المساعدة المحضرة.

تم اعداد دراسة نظرية شاملة تضمنت انشاء وتطوير موديل رياضي يصف ديناميكية التفاعل لعملية التهذيب بالعامل المساعد لمادة النفثا الثقيلة. الموديل الرياضي يصف توزيع تراكيز المواد المتفاعلة والناتجة، نسبة التحول، وتوزيع درجة الحرارة مع الزمن ومع طول المفاعل. أثبتت النتائج وجود تطابق كبير بين النتائج العملية للبحث والنتائج النظرية ونسبة أنحراف تتراوح بين (1.93 % - 14.51%).

مفتاح المصطلحات: دراسة تجريبية ونظرية(محاكاة) لعملية التهذيب، ($Pt\text{-}Sn/AL_2O_3$ and $Pt\text{-}Ir/AL_2O_3$).